Monitoring Earthquake-Induced Loading with Camera Networks: Case Study in Sherman Oaks, California

Tara C. Hutchinson[1], Derek Nastase[1], Samit Ray Chaudhuri[1], Rebecca Chadwick[1], Kai-Uwe Doerr[2], and Falko Kuester[2]

[1]Department of Civil and Environmental Engineering, University of California at Irvine, USA
[2]Department of Electrical Engineering and Computer Science, University of California at Irvine, USA

ABSTRACT

The advent of high speed, CCD-based camera technologies opens new possibilities for field monitoring applications. In particular, under natural or man-made loading conditions, applying these new technologies towards the monitoring of building interiors may substantially help rescue and reconnaissance crews during post-event evaluations. To test such a methodology, we have developed a specialized network of high-speed cameras and supporting hardware for monitoring and tracking nonstructural elements subjected to vibration loading, within building structures. Teamed with the University of California, Los Angeles, a full-scale vibration experiment is conducted on a vacant structure damaged during the 1994 Northridge Earthquake. The building of interest is a four-story office building located in Sherman Oaks, California. The investigation has two primary objectives: (1) to characterize the seismic response of an important class of equipment and building contents and (2) to study the applicability of tracking the response of these equipment and contents using arrays of image-based monitoring systems. In this paper, we describe the image acquisition (hardware and software) system and the experimental field set-up are described. In addition, the underlying communication, networking and synchronization of the camera sensor system are discussed.

Keywords: Motion tracking, field monitoring, camera calibration, synchronization, image acquisition, nonstructural elements

1. BACKGROUND AND INTRODUCTION

Natural disasters such a earthquakes place reconnaissance and rescue teams in the difficult position that all affected buildings have to be evaluated for their level and type of sustained damage, overall structural integrity and ultimately accessibility for rescue attempts. First responders are faced with a daunting task, considering the combination of possible aftershocks, uncertainty about conditions within the building and risk of secondary effects such as fires in combination with a lack of information about where aid is most urgently needed. Often it is dangerous for rescue workers to enter a building to rescue a person, and sometimes more difficult to determine where that person is located. In addition to incidences of collapse, rescue workers may have to rummage through furniture and overturned equipment in their searches. Long hours necessary to carry out such searches reduce the effectiveness of their efforts, as victims often cannot survive long after the event. Unfortunately, very little is known about the behavior of internal elements of the structure (nonstructural elements and building contents), which are the major cause of delay in rescue operations.

Within a building, nonstructural elements are components that are not considered part of a force resisting system. Generally, building components that are not designed within the structure are considered the responsibility of the building owner or tenants.[1] While the primary structure of a building may perform well in an earthquake, it is very likely that extensive nonstructural damage will occur, resulting in unnecessary life safety risks and excessive economic losses. Combining the lack of design information with the lack of existing mitigation strategies, nonstructural elements pose a problem to both life safety and economic recovery efforts.

Failure of small nonstructural components, such as water pipes and electric lines, can discontinue business operations, resulting in significant economic losses. The effect of business disruption trickles down as projects discontinue and services

Corresponding Author – T.C. Hutchinson, E-mail: thutchin@uci.edu, Telephone: 1-949-824-2166.

are stopped, resulting in the loss of wages and employment. Urban areas are particularly susceptible to these types of losses. For example, in a magnitude 7.0 earthquake scenario on the Hayward fault in the San Francisco Bay, an approximate $1.3 billion in commercial and industrial building disruptions[2] might be expected. Loss of nonstructural components is not limited to the United States, as demonstrated by the 1995 Kobe Earthquake in Japan. The Hyogo Prefecture, which was impacted by the Kobe quake, is responsible for nearly 4% of the gross national product that was brought to an economic standstill.[3]

A pervasive issue precluding advancement of our understanding of nonstructural components is the large number and type of such elements. Naiem notes that with such a large number of specific components in the nonstructural category, blanket design specifications are impossible.[1] Within the large variety of items, one specific area is especially critical; the damage of elements containing hazardous materials. Damage to these elements creates an immediate risk to people within the building, making post-earthquake risk assessment a dangerous and difficult task. During the 1994 Northridge Earthquake, 387 hazardous material incident occurred, of which nearly 60% occurred within laboratories.[4] Clean up of the hazardous material spills cost an estimated $1.5 million. Following the Northridge earthquake, a consortium of engineers and researchers in the United States developed documents to assist in the rehabilitation of existing buildings. These documents, which are provided to the public by the Federal Emergency Management Agency (FEMA), include commentary on the repair needed to several key nonstructural elements, including hazardous material storage devices.[5] Despite the recommendations of this document, design standards are still non-uniform and limited due to a lack of research in this area. The movement of expensive nonstructural elements, especially within hazardous substance laboratories (computers, microscopes, etc.) cannot be predicted at the current time, and their mitigation is therefore haphazard at the least.

The large diversity of nonstructural elements, with varied purposes, increases the complexity of even gaining a basic understanding of their behavior. To understand nonstructural element behavior, one needs to observe the three dimensional response of an object in varied conditions under a variety of motions. However, traditional methods of monitoring their behavior, from the Civil Engineering perspective, render 3D response measurement difficult, as typically discrete, point-wise measurement instruments are used. An alternate methodology is necessary to pursue the problem more thoroughly such that nonstructural behavior can be accurately interpreted. Ground based sensor networks and high-end computing technology are now emerging as tools that can support the real-time monitoring of structures in and after seismic events.

2. SCOPE OF THIS WORK

The advent of high speed, charged-couple-device (CCD)-based camera technologies opens new possibilities for field monitoring applications. Applying these new technologies towards the monitoring of building interiors may substantially help rescue and reconnaissance crews during post-event evaluations. To test such a methodology, a specialized network of high-speed cameras and supporting hardware for monitoring and tracking nonstructural elements subjected to vibration loading, within building structures is described in this paper. Teamed with the University of California, Los Angeles, a full-scale vibration experiment is conducted on a vacant structure damaged during the 1994 Northridge Earthquake. The building of interest is a four-story office building located in Sherman Oaks, California. The investigation has two primary objectives: (1) to characterize the seismic response of an important class of equipment and building contents and (2) to study the applicability of tracking the response of these equipment and contents using arrays of image-based monitoring systems. In this paper, we describe the image acquisition (hardware and software) system and the experimental field set-up.

2.1. Field Building Experiment in Sherman Oaks, California

The building of interest, known as the Four Seasons Office Building, was yellow tagged and condemned after the Northridge Earthquake in 1994. The primary component rendering the building unsafe was a number of damaged gravity columns, which punched through the floor slabs at several locations throughout the building. Punching shear failure, as it is called, is a result of the inability of the floor slab to transfer forces into the column. The Four Season's Building was constructed with a flat-slab and column capital system, designed to perform as gravity load resisting members, with no consideration for transferring lateral seismically-induced loads. In this case, beams are not used to span between interior columns within the building. A detail of the flat slab column connection is shown in Figure 1(a) and a photograph of a typical punching shear failure observed in the building is shown in Figure 1(b).

Approximately 9 kilometers from the earthquake epicenter, the Four Seasons building was built on a region of alluvial soil in Sherman Oaks, California. A nearby Cal Fed building, approximately 1.5 kilometers from the Four Seasons' Building, contained acceleration sensors that were monitored by the United States Geological Survey (USGS). Ground

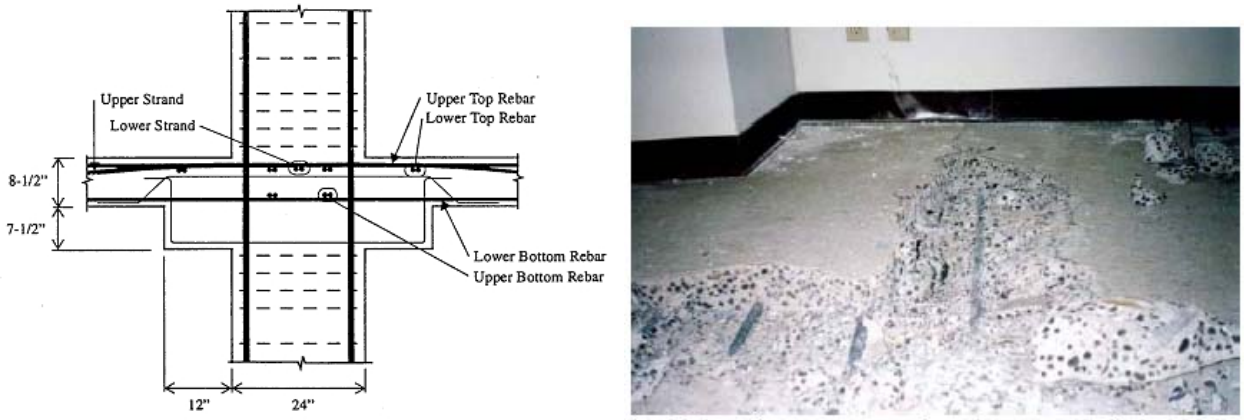

(a) (b)

Figure 1. Punching slab failure: (a) architectural detail of the flat slab-column connection, and (b) photograph taken in the Four Seasons Building.

motions recorded here, showing maximum accelerations of 0.8g along the short axis of the building, are a reasonable representation of the likely ground motions experienced by the Four Seasons' Building.

2.2. Vibration Testing

A research team from UCLA conducted full-scale vibrational tests on this structure by mounting linear and eccentric mass shakers to the roof of the building using NEES* mobile testing equipment. Vibration and monitoring system control was conducted from the exterior of the building in a vacant parking area (Figure 2(a)). Shakers were designed to induced excitations varying from step-functions, to scaled versions of actual ground motions, operating in both north/south or east/west (translational) and torsional (twisting) modes (Figure 2(b)).

(a) (b)

Figure 2. The Four Seasons building: (a) photograph of exterior of building and (b) photograph of two shakers mounted on the roof of the building (linear shaker shown in the foreground, eccentric shaker in the background).

*NEES is the Network for Earthquake Engineering Simulation

While the team from UCLA studied the building structure, the UC Irvine team developed an interior building monitoring strategies. Recreating three envisioned laboratory rooms on the fourth floor of the building, high speed camera systems coupled with analog instruments and networking equipment, were used for monitoring these laboratories (denoted 1-3 in Figure 3). The selection of room locations within the Four Seasons' Building was intended to maximize the possible input floor motion. Therefore, Rooms 1 and 3 were selected at the extremes of the building, near to the eccentric mass shakers, since the maximum floor level motion was anticipated to occur at the extreme ends of the building, due to torsionally-induced loading. Room 2 was selected in a location near to the linear mass shaker, roughly in the middle of the building.

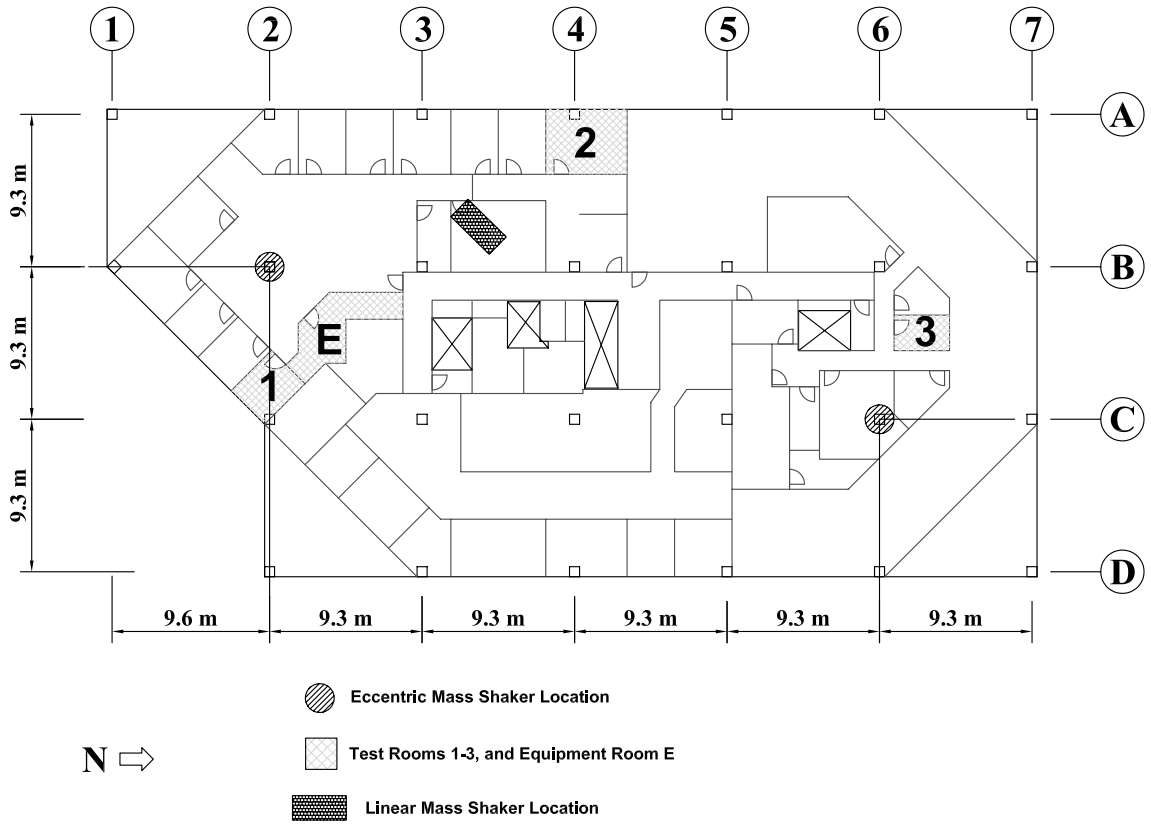

Figure 3. Plan view of the Fourth Floor in the Four Seasons Building.

2.3. Nonstructural Items of Interest in this Study

There are numerous types of nonstructural systems performing various roles within the interior of building structures, however, we focused on items commonly found in hospitals and/or science research laboratories. The interior laboratories within these buildings are critical to the occupants and the primary activities the structure supports. A particularly vulnerable example are science laboratories on University campuses. These campuses contain highly concentrated research facilities, therefore damage to their facilities cripples the productivity of entire campus. On the University of California, Berkeley (UCB) campus, for example, laboratories occupy 30% of the overall usable space on the campus, resulting in 50% of the research being conducted in seven out of 114 buildings. Even more critical is the research supported by these facilities, for the UCB campus, Comerio[6] noted that 72% of the approximately $400 million in research funding per year is concentrated within the science and engineering disciplines. Laboratory contents within these buildings is estimated at $676 million (21% of the total insured assets for the UCB campus).[7] For a UCB case study building, Comerio[8] found that 98% of all equipment within the building was valued between $1,500 - $10,000, while the remaining 2% ranged in value from $10,000 - $1 million. The result is a space valued between $200 - $300 per ft^2 (typical office space is approximately

$25 per ft^2). Content within these laboratories are not only valuable and important to the researchers, they often contain hazardous chemicals, posing operational and life-safety threats.

Specific types of equipment housed in these buildings include scientific instruments such as analyzers, microscopes, centrifuges, monitors, and computer workstations. In general, these equipment are short and rigid, therefore, imposed seismic excitation results in a sliding-dominated, rather than a rocking-dominated response.[9] Upon sliding, there is concern that the equipment may be damaged either by falling from the supporting surface or through impact with neighboring equipment or surrounding sidewalls. Previous experience by the authors led to the selection of a set of nonstructural elements for use in the field tests. The larger categories of these included; science equipment, expensive graphics computers, and small glassware. The frictional resistance of these elements was characterized, using controlled laboratory tests.[10] Of the previously tested equipment, only items with low frictional resistance were selected for use in the field testing, to assure movement during vibration loading.

In science laboratories or hospitals, these equipment are generally placed on the surface of ceramic laboratory benches, which in turn are attached to the structural floor and ceiling systems. Since the sliding of the equipment will be initiated when the acceleration at the top of the supporting element overcomes the resistance due to friction between the two surfaces of contact, considering the acceleration amplification due to a support element (such as a bench or shelf furnishing) is also very important. Considering this configuration, obtaining the resulting bench- or shelf-mounted equipment response requires a cascade style analysis. In this case, the ground input motion is propagated through the building to the floors, then through the supporting element (in this case, a bench is shown), to obtain estimates of the input motion at the bench-top. In this sense, the recreation of the a realistic equipment support structure (bench-shelf system) is important.

Typical bench-shelf systems are attached to the building with a uni-strut railing systems, resulting in a pinned support at the floor and ceiling to anchor the bench, creating a system with some flexibility. The result may be that the natural frequency of the laboratory bench lies within the acceleration sensitive zone of the input floor response spectrum, and may therefore experience acceleration amplification. Testing of typical uni-strut supported bench-shelf systems in the laboratory indicates their fundamental frequency is between f_n = 10 to 16 Hz.[9] Although transmissibility functions can easily be generated for the support structures, since the sliding response of the equipment is nonlinear, it is not possible to determine the response of the equipment by simply scaling the input acceleration to account for the bench amplification. This has also been observed by other researchers [e.g. Shao and Tung[11] and Garcia and Soong[12]]. Therefore, to calibrate sliding response models for equipment mounted on furnishings, it is important to consider the dynamic characteristics of the entire system (building, bench, equipment-interface). Thus, a field study accounting for each of these elements will provide a more thorough understanding of the time varied nonlinear sliding movement of the equipment.

2.3.1. Specific Design of Nonstructural Systems in Building Experiment

Using donated equipment and materials from UC Berkeley, the three separate laboratory rooms were constructed. Typical science laboratories are constructed of bench and shelf system furnishings. In the field, these systems consist of a series of cabinets with ceramic countertops with box shelving above, all of which is supported by a uni-strut steel grid. The uni-strut system, which is meant for quick construction and portability, mounts at both the floor and ceiling, creating a flexible, but sturdy support system. These bolted connections tied into the concrete slab on the fourth floor and roof levels. Sample photographs of the details and configurations constructed in the field are provided in Figure 4(a)-(c). Note the uni-strut system consisted of three vertical, double width pieces, and three horizontal pieces, all of which are pin connected to one another. The upper shelf system is connected to the top two horizontal pieces, whereas the bench (lower) portion is connected to one of the horizontal uni-struts and resting on floor. Pieces of equipment were typically placed on the benchtop area, or within the upper shelves. The three rooms varied in configuration in three ways; orientation, the number of bench-shelf systems (either one or two), and slight dimensional differences.

In addition to the laboratory set-ups monitored within the building, the dynamic response of other nonstructural elements was measured as well. Figure 5 provides photographs of a roof-level compressor (part a) and a multiply-supported piping system that were outfitted with seismic accelerometers. The roof compressor rested on a spring base, while the piping system extended along the length of the fourth floor ceiling (below roof).

2.4. Monitoring System

Figure 6 provides a schematic layout of the monitoring system developed for this work. The complexity of the system was enhanced, compared with an in-service building subjected to a real earthquake, due to the following factors: (i) for

(a) (b) (c)

Figure 4. Typical bench-shelf details: (a) horizontal-vertical connections, (b) back-to-back, and (c) single bench-shelf systems.

(a) (b)

Figure 5. Other nonstructural elements monitored in building: (a) roof compressor and (b) drainage piping system

safety reasons, testing crew were not allowed in the building during testing, (ii) due to the multiple data types used, the information gathered had to be time synchronized, and (iii) power was not available in the building. Without a testing crew allowed in the building during testing, our systems had to be activated remotely, hence the usage of a wireless network.

Each room contained a data acquisition computer system, four cameras, and a set of analog sensors (Table 1). Analog sensors were wired and collectively run into a analog-to-digital convertor, then into a data acquisition PC, which was stored in an equipment room. Within the building, all of the computer systems were routed into a network box, which was in turn connected to a wireless base station that communicated with the computer systems outside of the building. Despite the limited range, the system was effective in running and monitoring the data collection process. For an added element of security and monitoring, web cameras were placed in each of the rooms for active monitoring, insuring that all of the system remained intact during vibration. A NTS 150 GPS time server was used in the fourth floor network, synchronizing each Window's system clock to an accurate global time acquired by an antenna placed on the building's balcony. The time synchronization insured that data collected from the analog and camera systems could be compared with one another,

and also with data collected by UCLA. Finally, the lack of power in the building was resolved by providing a gas-driven, Honda inverter generator, also left on the balcony to allow the ventilation of the exhaust. Details of the data recording system equipment is provided in Table 1.

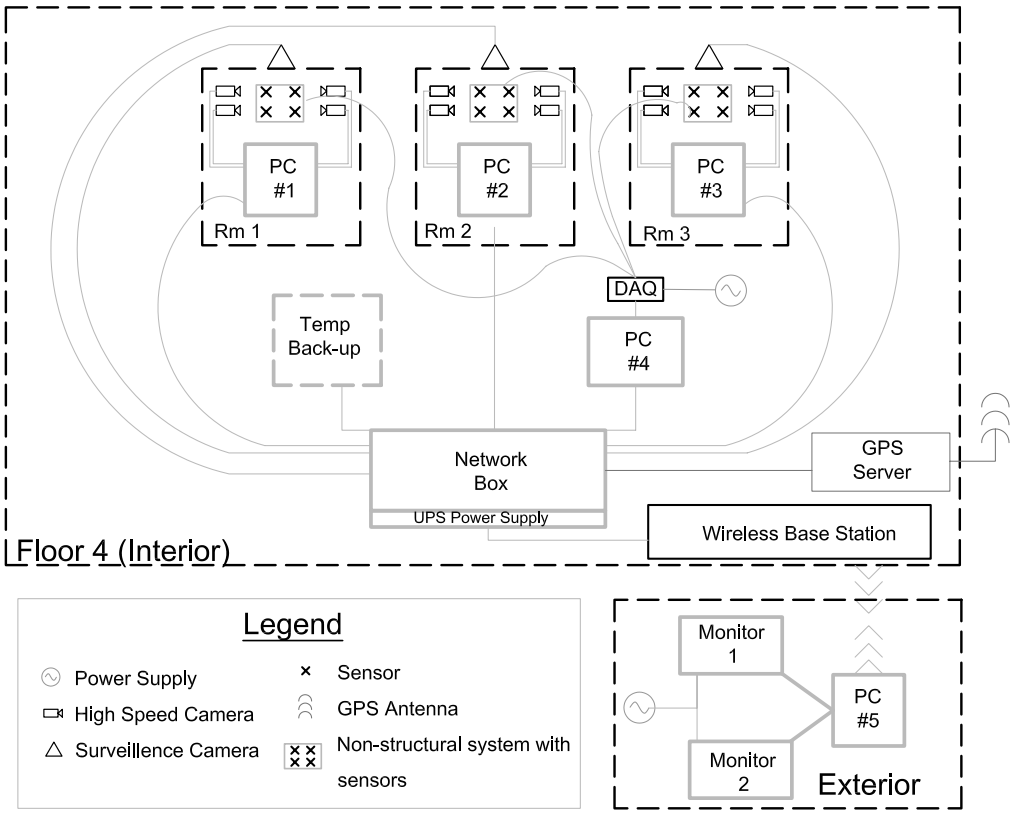

Figure 6. Schematic of the monitoring system design for the Four Seasons Building.

The motion recording system acquired two separate inputs, the visual images of the camera system, and the analog data records from the analog sensor system. The camera system consisted of four Basler A301fc cameras per room connected to a data acquisition computer (denoted PCs #1,2, and 3), with each system remotely controlled through the network box and wireless network. The analog system consisted of a series of sensors placed in each rooms' laboratory setup, and connected to the data acquisition system (DAQ), which was also networked to be controlled via wireless network.

2.5. Analog Instrumentation Layout

Two different types of analog sensors were used in these experiments; accelerometers and string potentiometers. Accelerometers were placed at the floor and roof levels, near each of the monitored rooms, to determine the relative acceleration imposed between the floor of interest. In each room, bench countertops and shelves were also instrumented with accelerometers. Figure 7(a) schematically shows a typical accelerometer layout within a room and as placed on the bench-shelf system.

String potentiometers were placed on the countertops to measure the displacement of specific pieces of equipment. The photograph shown in Figure 7(b) shows a typical layout using three string potentiometers attached to a computer. Three string potentiometers per piece of equipment allowed the determination of its three degrees of motion in plan (translation in the x and y directions, and rotation).

Item	Manufacturer (Part No.)	Quantity	Function	Specification
Uni-axial Sensors	PCB Piezotronics (393B04)	14	Monitor local accelerations	5g max., 0.001g resolution
String Potentiometers	Patriot Sensors and Controls Corp., Rayelco Linear Motion Transducer	9	Monitors displacement and rotation (across multiple sensors)	49.77mV/V/in precision, +/-10" stroke,
16 Channel ICP Source	PCB Piezotronics	1	Maintains constant voltage for the accelerometers	(+/-)5V source for accels (16 Channel ICP)
Camera Lenses	Canon	8	Focus the cameras	4.8mm, F1.4, C mount
Camera Mounting	Constructed in-house	12	Steady, yet changeable positioning of cameras	3 DOF flexible rotation mount
Global Positioning Satellite (GPS) Time Server	Symmetricom (NTS-150)	1	Collects GMT from satellites and adjusts the Windows clock to precise time	12 channel GPS Receiver, 10/100 Base Ethernet, accuracy <1 µsec
CCD Cameras	Basler (A301fc)	12	Capture images within a subregion of a room for later analysis	80fps at 658x494 resolution
Power Generator	Honda (EU2000i)	1	Power source for the entire Fourth floor system	1600W, 12V, 4hr power supply at rated load
Surveillance Cameras	Micro USB	3	Observe the scenes remotely to guard against unwanted damage	25 to 30fps at 352x288CIF resolution
PC# 1-3	Monarch (Intel Xeon 4U SCSI/RAID)	3	One PC per room running the camera acquisition software	Server style, 4x36Gb hard drives
PC# 4	Hewlett-Packard (Pavillion 743c)	1	Analog data collection PC	70 Gb and 5 Gb hard drives
PC# 5	Toshiba	1	Control from outside the building	Notebook PC, 20Gb Hard Drive
Wireless Router	LinkSys (VRT 546)	1	Wireless connection to the network inside the building	2.4 GHz BB, 4 port, 54 Mbps
Network Box	SMC (Easy Switch 1000)	1	Network all computers within the Four Seasons' Building together	6 inputs, 2 uplinks
UPS Power Supply	CyberPower(1500AVR)	1	Back-up power source	12A output, 125V input
Temporary Back-Up Drive	Iomega (HDD 250 Gb)	2	Back-up data storage	250 Gb capacity, Firewire and USB enabled

Table 1. Function and specifications of equipment used for monitoring system in the Four Seasons Building.

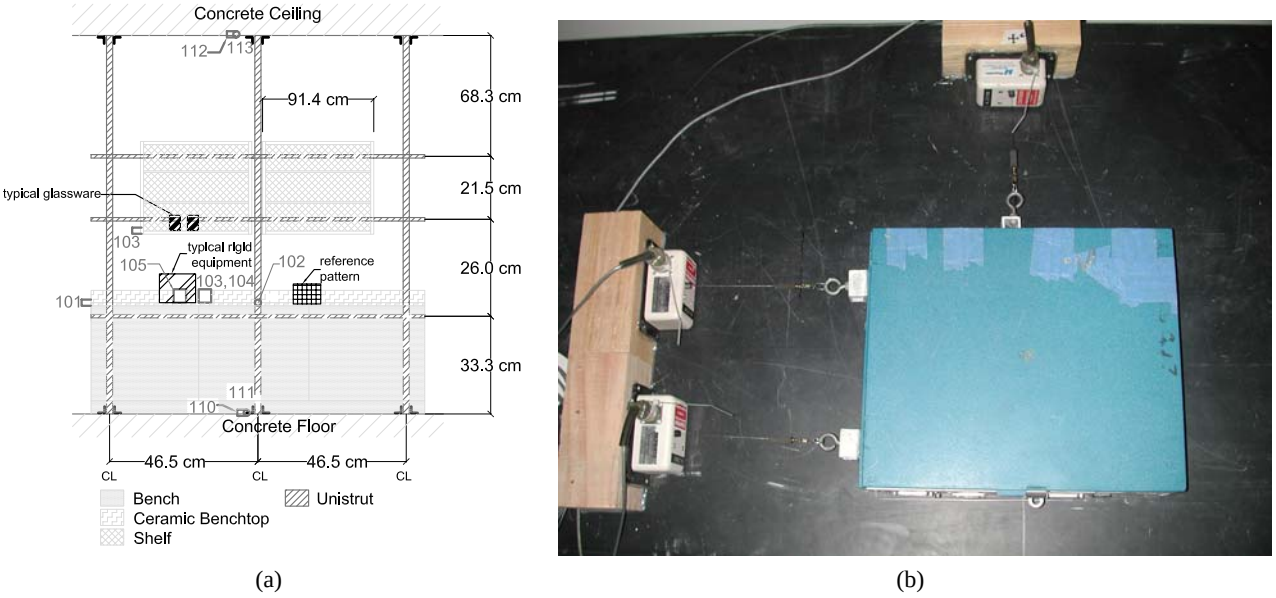

(a) (b)

Figure 7. Analog instrumentation details: (a) schematic of bench-shelf system instrument locations and (b) typical displacement transducers placed on bench-top equipment.

2.6. Camera System

Four high speed cameras, with a resolution of 658x496 and capturing at a rate of 80 frames per second (fps) were placed in each room for dynamic monitoring. 3-dimensional camera mounts were designed to flexible placement during experiment preparation (Figure 8(a)). As shown in Figure 8(b), cameras were mounted on the wall on a plywood backing plate and arranged in a T- or corner square pattern. They were placed such that each camera viewed the same scene, from a different location, so that 3-dimensional movement could be reconstructed and arbitrary camera position could be back-calculated. A reasonable field-of-view of the equipment and a portion of the bench-shelf system was obtained (Figure 8(c)).

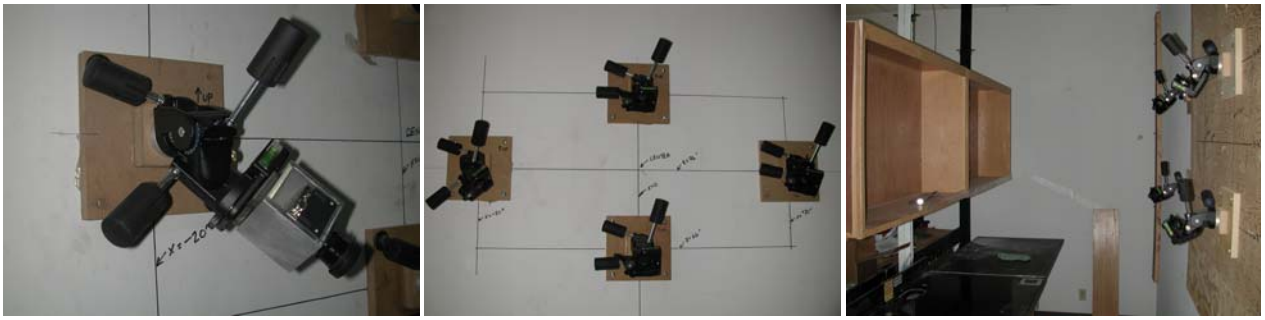

(a) (b) (c)

Figure 8. Camera photographs: (a) 3-dimensional camera mount, (b) four camera arrangement, and (c) viewing scene of camera array.

2.7. Input Motions

Building interior monitoring was conducted during specific events, when the magnitude of the motion would reach levels high enough to move the equipment. Table 2 provides a summary of the test data collecting, including total duration of sampling and details about the input motion used. A total of 12 series of motions were recorded, including sin waves, white noise, and scaled down versions of motions recorded during the Northridge earthquake. Of these ground motions, the largest acceleration was produced in the torsional motions.

Name	Date	UCI Recording Time	UCI Total Duration (sec)	Total Duration (sec)	Description
Linear-Shaker, Sine Sweep	07/19/04	13:50:00	327.465	2:30:06	Linear Shaker with Sine Sweep
Linear-Shaker, White Noise		14:54:00	122.025	2:30:06	White Noise input record
Mass Shaker, Torsional 1		15:32:00	887.490	2:30:06	Eccentric Mass Shaker, Torsional Motion 1.
Mass Shaker, Torsional 2		16:12:00	2182.330	2:30:06	Eccentric Mass Shaker, Torsional Motion 2.
Mass Shaker, Translational 1		15:18:00	1886.100	2:30:06	Eccentric Mass Shaker, Translational Motion.
Translational North South, Trial 1	07/22/04	14:12:00	827.165	1:16:47	North and South Motion, Eccentric Mass Shakers, translation (aborted)
Translational North South, Trial 2		14:45:00	1259.710	1:16:47	North and South Motion, Eccentric Mass Shakers, frequency step, translation
Translational North South, Trial 3		15:11:00	176.720	1:16:47	North and South Motion, Eccentric Mass Shakers, linear sine sweep (aborted)
Translational North South, Trial 4		15:15:00	179.815	1:16:47	North and South Motion, Eccentric Mass Shakers, linear sine sweep
Translational North South, Trial 5		15:22:00	244.380	1:16:47	North and South Motion, Eccentric Mass Shakers
Eccentric North South, Trial 1	07/28/04	16:32:00	1398.245	9:52:00	Eccentric mass shakers in the NS direction
Eccentric Sweep up to 4Hz, Trial 1		16:56:00	420.290	9:52:00	Eccentric mass shaker sine sweep up to 4 Hz
Linear Shaker, Earthquake Motion 1		15:00:00	115.830	9:52:00	Linear Shaker with Northridge Earthquake motion, scaled down
Linear Shaker, Earthquake Motion 2		15:03:00	124.870	9:52:00	Linear Shaker with Northridge Earthquake motion, scaled down
Linear Shaker, Trial 1		15:07:00	405.800	9:52:00	Linear Shaker, white noise
Linear Shaker, Trial 2		15:16:00	439.510	9:52:00	Linear Shaker, white noise
Linear Shaker, Trial 3		15:31:00	412.865	9:52:00	Linear Shaker, white noise
Eccentric_Sweep_upto4Hz	08/02/04	13:06:00	501.090	3:20:47	In the NS direction with one eccentric mass shaker, a sine sweep upto the 4 Hz level, and maintained.
Eccentric_3Hz		13:25:00	1502.175	3:20:47	Began the collection 45 seconds early, NS direction with both shakers, rapidly ramp up to 3 Hz and held at that point.
Acc Sweep 5 Hz		14:01:00	1323.160	3:20:47	2 runs of the linear shaker, sweeping up to 5 Hz with a sine wave motion.
Step Function 0 to 4.25Hz	08/03/04	10:35:00	2720.820	1:58:39	In the EW direction with both eccentric mass shakers, with 18 steps, held at 4.25 Hz for a prolonged period of time.
Fast Ramp up to 4.25Hz		11:41:00	665.565	1:58:39	Also in EW, with both eccentric mass shakers, although run mare quickly up to the 4.25 Hz level.

Table 2. Detail information about the different motions applied to the Four Seasons' Building.

3. IMAGE PROCESSING ALGORITHMS: PIXEL-BASED IMAGE PROCESSING CHAIN (PIPC)

In this section, we describe the actual processing applied to the images and the data analysis steps undertaken to track dynamic movements in the scene. Image processing and data analysis is realized using a pixel-based motion detection approach, whereby pixels identify objects and features. For both motion detection and object recognition tasks, we use and extend the Open Source Computer Vision Library (OpenCV).[13] The general outline of the **p**ixel-based **i**mage **p**rocessing **c**hain (PIPC) implemented in this work is illustrated in Figure 9. This analysis is applied sequentially for all images in a given video stream.

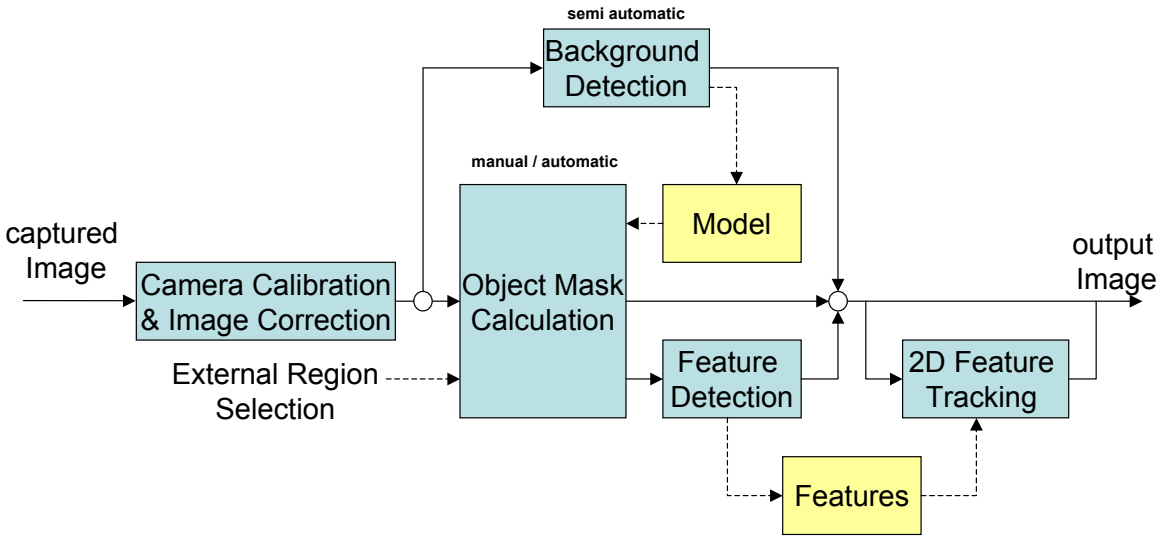

Figure 9. Pixel-based image processing chain (PIPC) flowchart.

The process begins with camera calibration and correction of the image, particularly for radial and tangential distortions introduced by the camera lens. A complete review of camera calibration fundamentals and techniques applied is provided by Villa-Uriol et al.,[14] therefore, no further discussion of these techniques is warranted. Subsequently, to identify trackable objects in the scene and to reduce computation time, we use a mask-based object identification approach. The object mask can be determined either by user-defined regions in the acquired image, or by referencing an image to a precalculated model of the clean background. Features of interest are then identified within the object mask in each image. Feature data sets are then stored and passed to a 2-dimensional (2D) feature tracking algorithm. The implemented feature tracking algorithm is based on the calculation of the optical flow of pixel values in an image sequence.

3.1. Feature Detection within Object Masks

In our processing pipeline, (Figure 9), either predefined regions (manual) or the difference between the background model and new images (semi-automatic) are used to define an *object mask*. Within this object mask, features are subsequently identified and tracked. The *semi-automatic* feature detection method is intended to automatically identify *good features* to track within a user definable ROI.

The general structure of the feature detection method is based on the work by Shi and Tomasi.[15] This method searches for corners with large eigenvalues in the image and returns a number of features based on two user definable parameters: (i) the desired quality of a detected feature and (ii) the minimum distance between two nearby features. It can be expected that many features would normally be detected that are not part of the moving object. To reduce the overall feature set, and hence the computation time, the background mask is used to focus on features located specifically on the moving object. The result is that elements not located within the object mask are not identified as features to track.

3.2. 2D Feature Tracking

Once object features are detected, they are tracked with a set of optical flow algorithms. The optical flow is defined as an apparent motion of image brightness over time (image frames). Two main assumptions were made to establish a set of boundary conditions: (i) a feature pixel $p(x,y)$ in an image I_t at time t has minimal movement between two consecutive images, allowing feature pixel $p(x,y)$ to be identified within the same region of image $I_{(t+1)}$ and (ii) the brightness of each point of a moving or a static object does not change over time. The *optical flow constraint equation* establishes the basic formulation for all optical flow functions:

$$-\frac{\partial I}{\partial t} = \frac{\partial I}{\partial x}u + \frac{\partial I}{\partial y}v \tag{1}$$

where, the variables u and v are the components of the optical field in the x and y directions, respectively. For our process chain, the technique of Lucas and Kanade[16] was used.

The basis for the Lucas and Kanade implementation is the minimization of a residual function, based on the image velocity d. If an image point is defined by $u = [u_x, u_y]^T$ on the initial image I, the feature tracking goal is to find the location $v = u + d = [u_x + d_x, u_y + d_y]^T$ on the subsequent image J such that $I(u)$ and $J(v)$ are similar. The vector $d = [d_x, d_y]^T$ is the image velocity at a pixel point $p(x,y)$, also known as the optical flow. Due to the *aperture problem*, it is essential to define the notion of similarity in the context of a 2D neighborhood. In this context, the image velocity d can be defined as a vector that minimizes the residual function ε:

$$\varepsilon(d) = \varepsilon(d_x, d_y) = \sum_{x=u_x-w_x}^{u_x+w_x} \sum_{y=u_y-w_y}^{u_y+w_y} (I(x,y) - J(x+d_x, y+d_y))^2 \tag{2}$$

where, w_x and w_y are integer values that define the window size for the neighborhood search.

The algorithm first searches in a given window area around the actually processed pixel and tests for similarity. If the point falls outside the image or if the image patch surrounding the tracked point varies too much between image I and image J, the result will be features that are lost. If the internal threshold value for ε cannot be reached during the optical flow calculation, a feature will also be marked as lost.

We also achieve sub-pixel accuracy by using the optical flow method in combination with a cornering function. This method is based on the observation that every vector from the center q to a point p located within a neighborhood of q is orthogonal to the image gradient at p subject to image and measurement noise. Therefore:

$$\varepsilon_i = \nabla I_{p_i}^T \cdot (q - p_i) \tag{3}$$

where, ∇I_{p_i} is the image gradient at one of the points p in a neighborhood of q. The value of q is found by minimizing ε_i. Consequently, a system of equations can be found by setting each ε_i equal to zero:

$$\left(\sum_i \nabla I_{p_i} \cdot \nabla I_{p_i}^T \right) \bullet q - \left(\sum_i \nabla I_{p_i} \cdot \nabla I_{p_i}^T \cdot p_i \right) = 0 \tag{4}$$

where, the gradients are summed with a neighborhood (”search window”) of q. By defining the first gradient as G and the second gradient as b, q can be expressed as $q = G^{-1} \cdot b$. The algorithm sets the center of the neighborhood window at this new q and then iterates until the center stays within a set threshold.[13]

4. SUMMARY REMARKS AND CONCLUSIONS

Under natural or man-made loading conditions, applying newly developed sensor technologies towards the monitoring of building interiors may substantially help rescue and reconnaissance crews during post-event evaluations. To test such a methodology, we have developed a specialized network of high-speed cameras and supporting hardware for monitoring and tracking nonstructural elements subjected to vibration loading, within building structures. Teamed with the University of California, Los Angeles, a full-scale vibration experiment is conducted on a vacant structure damaged during the 1994 Northridge Earthquake. The building of interest is a four-story office building located in Sherman Oaks, California. The investigation has two primary objectives: (1) to characterize the seismic response of an important class of equipment and building contents and (2) to study the applicability of tracking the response of these equipment and contents using arrays of image-based monitoring systems. In this paper, we describe the image acquisition (hardware and software) system and the experimental field set-up. Preliminary input motion and nonstructural system response data are being analyzed for different vibration loading cases and will be presented at the conference.

ACKNOWLEDGMENTS

Support for this work was provided by the National Science Foundation, Civil and Mechanical Systems Division (grant number 0340540), where Dr. Steven McCabe is our program manager. Assistance was provided by Mr. Bob Kazanjy, Development Engineer, and other research staff of the Structural Engineering Test Hall (SETH) and in the Visualization and Interactive Systems (VIS) Group at the University of California, Irvine. We thank Professor John Wallace and John Stewart at UCLA for inviting us to join in this unique field experiment. The above financial and other support is greatly appreciated.

REFERENCES

1. F. Naeim, ed., *The Seismic Design Handbook*, Kluwer Academic, 2nd ed., 2001.
2. EERI, "Scenario for a magnitude 7.0 earthquake on the Hayward fault," Tech. Rep. Publication no. HF-96, 1996.
3. "The january 17, 1995 kobe earthquake; an eqe summary report," website, EQE International, http://www.eqe.com/publications/kobe/economic.htm, April 1995.
4. EERI, "Northridge earthquake reconnaissance report vol. 1," *Earthquake Spectra* **Suplement C to Volume 11, Publication 95-03, Technical Editor J.F. Hall**, p. 523 pp, 1995.
5. FEMA, "Prestandard and commentary for the seismic rehabilitation of buildings – fema 356," tech. rep., Federal Emergency Management Agency, prepared by ASCE, Reston, Virginia, 2000.
6. M. Comerio, "The economic benefits of a disaster resistant university: Earthquake loss estimation for UC Berkeley," Tech. Rep. WP-2000-02, University of California, Berkeley. Institute of Urban and Regional Development, 2000.
7. M. Comerio, "Seismic protection of laboratory contents: The UC Berkeley science building case study," Tech. Rep. WP-2003-02, University of California, Berkeley. Institute of Urban and Regional Development, 2003.
8. M. Comerio and J. Stallmeyer, "Nonstructural Loss Estimation: The UC Berkeley Case Study," Tech. Rep. PEER-2002/01, Pacific Earthquake Engineering Research (PEER) Center, University of California, Berkeley, 2002.
9. T. C. Hutchinson and S. Ray Chaudhuri, "Bench-shelf system dynamic characteristics and their effects on equipment and contents," *Earthquake Engineering and Structural Dynamics* , 2004. (In Review).
10. S. Ray Chaudhuri and T. C. Hutchinson, "Characterizing frictional behavior for use in predicting the seismic response of unattached equipment," in *11^{th} International Conference on Soil Dynamics & Earthquake Engineering (SDEE)*, pp. 368–375, 2004.
11. Y. Shao and C. Tung, "Seismic response of unanchored bodies," *Earthquake Spectra* **15(3)**, pp. 523–536, 1999.
12. L. Garcia and T. Soong, "Sliding fragility of block-type non-structural components. Part 1: unrestrained components," *Earthquake Engineering and Structural Dynamics* **32**, pp. 111–129, 2003.
13. Intel Research Group, "Open Source Computer Vision Library," 2004. URL: http://www.intel.com/research/mrl/research/opencv.
14. M.-C. Villa-Uriol, G. Chaudhary, F. Kuester, T. C. Hutchinson, and N. Bagherzadeh, "Extracting 3D from 2D: Selection basis for camera calibration," in *7^{th} IASTED International Conference on Computer Graphics and Imaging (CGIM 2004)*, pp. 315–321, August 2004.
15. J. Shi and C. Tomasi, "Good features to track," *IEEE Computer Vision and Pattern Recognition* , pp. 593–600, 1994.
16. B. Lucas and T. Kanade, "An iterative image registration technique with an application to stereo vision," in *7th International Joint Conference on Artificial Intelligence IJCAI*, **April**, pp. 674–679, 1981.